Crystal orientation-ordered ZnS nanobelt quasi-arrays and their enhanced field-emission†

Xiaosheng Fang,* Yoshio Bando, Changhui Ye and Dmitri Golberg

Received (in Cambridge, UK) 11th April 2007, Accepted 15th June 2007
First published as an Advance Article on the web 26th June 2007
DOI: 10.1039/b705410f

Crystal orientation-ordered ZnS nanobelt quasi-arrays were fabricated using a non-catalytic and template-free thermal evaporation process; field-emission measurements show that these novel arrays are decent field emitters possessing a current density more than 20 times higher than that of randomly-oriented ZnS nanobelt ensembles at a macroscopic field of 5.5 V μm^{-1}.

Significant effort has been put into understanding the novel physical properties of one-dimensional (1D) nanostructures.[1–3] Field-emission (FE) is based on the physical phenomenon of quantum tunneling, during which electrons are injected from a material surface into vacuum under the influence of an applied electric field.[4] High-quality field emitters are desirable for applications in a wide range of FE devices. To date, various FE cold cathode 1D nanostructural materials have been developed such as C nanotubes, ZnO, Si, SiC, CdS and AlN nanowires, nanobelts and nanotubes.[5–8] It is well known that aligned nanostructures with a high packing density can significantly enhance the material FE properties.[9] ZnS, an important semiconductor compound of the II–VI group, has a wide bandgap energy of 3.7 eV at 300 K. ZnS is one of the first semiconductors discovered and probably one of the most important materials in the electronics industry.[10] Although intensive research has been focused on the fabrication of 1D ZnS nanostructures and exploration of their optical properties,[11–13] effective pathways towards ZnS FE property improvement have remained undiscovered.

In this communication, we describe a new strategy for the growth of quasi-aligned ZnS nanobelt arrays through a non-catalytic and template-free thermal evaporation process. The as-synthesized nanobelts were not only aligned on the micro/macroscopic scales but also displayed similar crystallographic orientation of their growth axes. FE characteristics of the aligned arrays were analyzed. These displayed a low turn-on field of $\sim$3.55 V μm^{-1} and a field-enhancement factor β of $\sim 1.85 \times 10^3$. The results suggest that the present oriented and well-ordered ZnS nanobelt arrays possess significantly enhanced FE characteristics compared to randomly distributed ZnS nanobelts. Most importantly, the observed FE properties may be comparable to or even surpass those of the above-mentioned pre-existing FE cold cathode materials, in spite of the fact that the work function for ZnS is larger than that in those materials. The measured emission current densities reached $\sim$14.6 mA cm^{-2} at a macroscopic field of 5.5 V μm^{-1}, that is more than twenty times that found for randomly oriented ZnS nanobelts. Therefore, the quasi-aligned ZnS nanobelt arrays may be attractive as practical field emitters.

Fig. 1 shows scanning electron microscopy (SEM, JSM-6700F) images of fabricated ZnS nanobelts. The observations reveal that a typical length of the belts is several tens-to-hundreds of micrometers. Some of them may even reach a millimeter in length. A low-magnification SEM image shown in Fig. 1(a) indicates that the belts are quasi-aligned. On zooming-in, perfectly parallel ensembles become visible, Figs. 1(b)–(d). A typical belt width is 50–120 nm. With an increase in the reaction temperature to 1150 °C, while keeping all other experimental conditions unchanged, ZnS nanobelt quasi-arrays with a coarse surface may be found. Figs. 1(e) and (f) show typical SEM images of a product synthesized at 1150 °C. The width and length of the nanobelts did not notably change.

The morphology and microstructures of the nanobelts were characterized using a JEM-3000F high-resolution transmission electron microscope (HRTEM) equipped with an X-ray energy

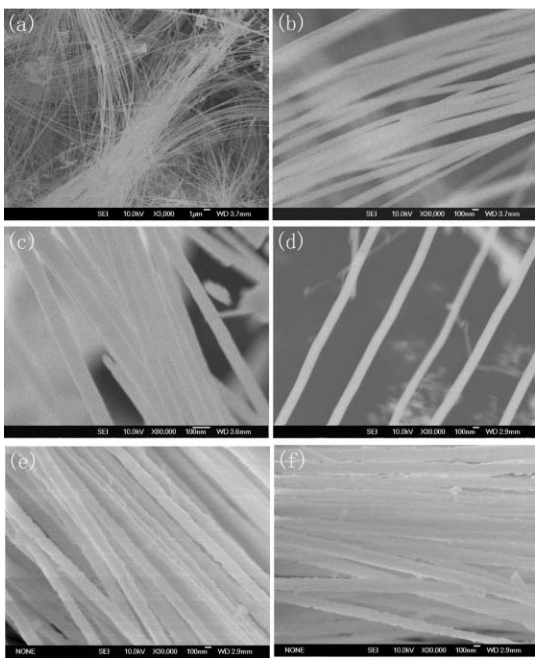

Fig. 1 (a) Low- and (b)–(d) high-magnification SEM images of a product, displaying quasi-aligned belt-like nanostructures; the nanobelts are nearly parallel to each other. (e) and (f) Typical SEM images of a product prepared after increasing the reaction temperature to 1150 °C.

Nanoscale Materials Center, National Institute for Materials Science, Namiki 1-1, Tsukuba, Ibaraki 305-0044, Japan.
E-mail: Fang.Xiaosheng@nims.go.jp; Fax: (+81) 29-851-6280
† Electronic supplementary information (ESI) available: Experimental section. See DOI: 10.1039/b705410f

dispersive spectrometer (EDS). Fig. 2(a) shows a typical TEM image of an array of the parallel nanobelts; this verifies the SEM results. The inset shows an electron diffraction pattern recorded from a bunch in Fig. 2(a). The similar orientation of all nanobelts within the bunch, that is along the $[001]_{ZnS}$ direction, is documented. This result is in accord with the determined crystal orientation in the ordered ZnS nanowire bundles synthesized through a two-step thermal evaporation process on Si(111) with CdSe as a buffer layer reported by the Wang group.[14] A TEM image in Fig. 2(b) clearly verifies a belt-like structure. No particles were observed at the ends of the nanobelts. Fig. 2(c) is a lattice-resolved HRTEM image taken from an individual nanobelt. It shows the (001) lattice plane of wurtzite ZnS with an inter-planar d-spacing of 0.62 nm, in accord with the [001] growth direction. The belts are free from defects. An EDS spectrum taken from a single nanobelt (Fig. 2(d)) confirms the stoichiometric ZnS composition of the material.

We found that a deposition substrate certainly plays the key role in the present nanobelt formation process. Wang *et al.*[14] and Zhu *et al.*[15] have respectively demonstrated that ordered ZnS nanowire bundles and assemblies could be controllably synthesized by growing a thin CdSe film onto a Si(111) substrate or by controlling the reaction temperature. Fan and co-workers[16] have achieved the orientation-controlled growth of single-crystal Si nanowire arrays by VLSE growth on a Si substrate. In this work, seeding ZnS sheets made of pressed ZnS nanoparticles offered numerous nucleation centers for the ordered nanobelt array growth. XRD measurements indicated that the used ZnS sheets had a polycrystalline wurtzite structure. Since both the ZnS substrate and the as-grown ZnS nanobelts have the same wurtzite structure, the epitaxial growth along the [001] direction seems to be the most energetically favorable process. ZnS clusters, generated in a higher temperature zone, are transported to the seeding ZnS sheets. The width of the nanobelts is almost unchanged under a synthesis temperature change; that is, always close to the size of a seeding ZnS nanoparticle, as shown in Figs. 1(e) and (f), indicating that the present ZnS seeding sheets, but not the reaction temperature or substrate temperature, certainly play the key role in the belt array formation.

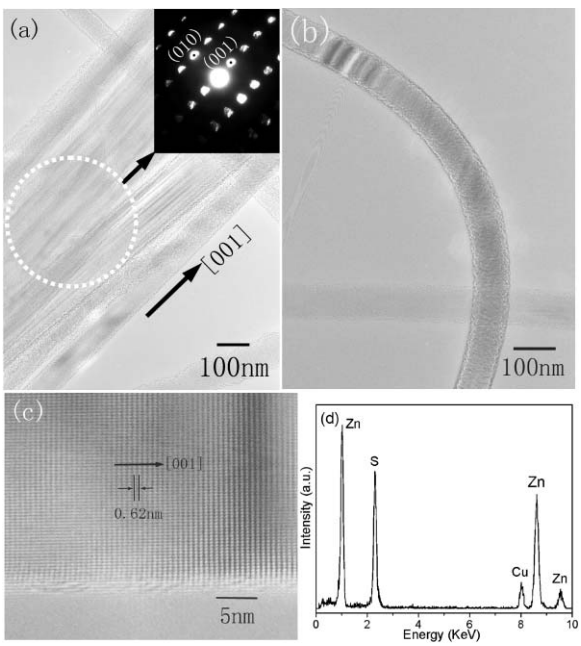

Fig. 2 (a) and (b) Typical TEM images of a ZnS nanobelt array and an individual ZnS nanobelt. The inset in (a) is the corresponding electron diffraction pattern taken from the bunch which shows uniform alignment along the $[001]_{ZnS}$ orientation. (c) A lattice-resolved HRTEM image (showing no lattice defects) taken from an individual nanobelt, confirming the [001] growth direction. (d) EDS spectrum taken from a single nanobelt revealing the stoichiometric ZnS composition.

The comparative plots of FE current density (J) *versus* applied field (E) for the films are depicted in Fig. 3(a). The inset in (a) is a magnified J–E curve for a randomly-oriented ZnS nanobelt film. The turn-on fields for the films made of ordered and random ZnS nanobelts were extrapolated as $\sim$3.55 and 4.19 V μm^{-1}, respectively, at a current density of 10 $\mu A\ cm^{-2}$. The emission current density reached $\sim$14.6 mA cm^{-2} at a macroscopic field of 5.5 V μm^{-1} for quasi-aligned and well-ordered ZnS nanobelt arrays. This value is more than 20 times higher compared to that of randomly distributed ZnS nanobelts (0.68 mA cm^{-2} at the same macroscopic field). The data suggest that quasi-aligned ZnS nanobelt arrays rival the previously reported FE cold cathode materials although the work function for ZnS is relatively larger.[17]

Fig. 3(b) shows the comparative Fowler–Nordheim plots for the films of aligned and random ZnS nanobelts; both fit well the linear relationship given by a simplified Fowler–Nordheim equation,[9,18]

$$J = (A\beta^2E^2/\phi)\ \exp\ (-B\phi^{3/2}/\beta E)\ \text{or}$$

$$\ln\ (J/E^2) = \ln\ (A\beta^2/\phi)\ -\ B\phi^{3/2}/\beta E$$

where $A = 1.54 \times 10^{-6}$ A eV V^{-2}, $B = 6.83 \times 10^3$ $eV^{-3/2}$ V μm^{-1}, ϕ is the work function of the emitting materials, which is 7.0 eV for ZnS.[20] β is the field-enhancement factor, which is related to the emitter geometry, its crystal structure, and spatial distribution of the emitting centers.

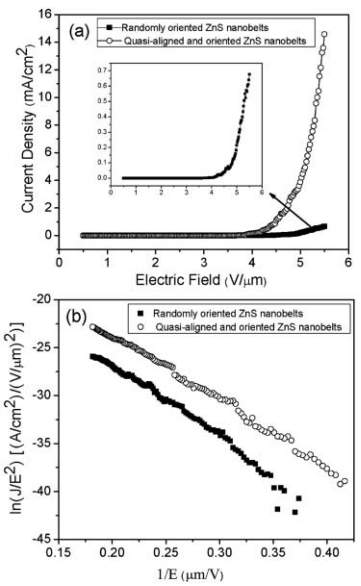

Fig. 3 Comparative FE properties of quasi-aligned ZnS nanobelt arrays, and randomly-oriented ZnS nanobelts. (a) J–E curves and (b) Fowler–Nordheim plots corresponding to (a). The inset to (a) is a magnified J–E curve of random ZnS nanobelts.

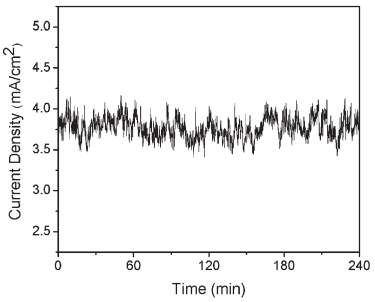

Fig. 4 A *J*–*t* plot of quasi-aligned ZnS nanobelt arrays when an applied electric field was 5 V μm^{-1}.

From the slopes of ln (J/E^2) – ($1/E$) plots in Fig. 3(b), the field-enhancement factors β of $\sim 1.85 \times 10^3$ and $\sim 1.60 \times 10^3$ were calculated for the ordered and disordered ZnS nanobelt ensembles, respectively. It is generally accepted that the field-enhancement factor of an individual nanobelt may be expressed as $\beta = l/r$,[9] where l and r are the length and thickness of the belt, respectively. Ren *et al.*[9,19] have demonstrated that the FE performance of ZnO nanowires/nanobelts can be significantly enhanced by increasing the field-enhancement factor *via* either changing the geometry configuration, decreasing the area density of the nanowires, or increasing the nanobelt aspect ratio. We have observed a similar phenomenon – the excellent FE performances could be achieved through increasing the aspect ratio of ultrafine nanobelts.[20] The length of the present ZnS nanobelts is up to several tens–hundreds of micrometers; their thickness is in the range of tens of nanometers. Therefore, it is logical that they possess excellent FE properties and high field-enhancement factors. It is also understandable that aligned structures with a high density can enhance the material FE properties as compared to those of random arrays.

Fig. 4 shows variations of emission current density of the ordered ZnS nanobelt ensembles within 4 hours at an applied electric field of 5 V μm^{-1}. The initial current density and the average current densities are 3.87 and 3.77 mA cm^{-2}, respectively. No notable current density degradation was observed, and the emission current fluctuations were as low as 2.58%, proving the high stability of ZnS aligned emitters. In general, a given FE device will exhibit poor stability if the emitter is not thermally stable, because much heat is generated when a high electric field is applied to it.[21] The stable FE performance discovered in this work is related to a uniform height of aligned ZnS nanobelts, which guarantees a uniform field distribution across the arrays.[18]

In summary, we have demonstrated an effective approach for the synthesis of quasi-aligned, well-ordered and crystallographically uniform ZnS nanobelt quasi-arrays. A ZnS pre-seeded deposition substrate has played the key role in the nanobelt alignment, which dramatically improves the array FE performance. The aligned arrays possess a low turn-on field of ~ 3.55 V μm^{-1} and a high field-enhancement factor β of $\sim 1.85 \times 10^3$. They also reveal an emission current density of ~ 14.6 mA cm^{-2} at a macroscopic field of 5.5 V μm^{-1} (which is more than 20 times higher when compared to randomly-oriented ZnS nanobelt ensembles). The arrays display good stability of the field-emission. All these properties make the aligned ZnS nanobelt ensembles highly valuable for novel nanoscale FE devices.

This work was financially supported by a Japan Society for Promotion of Science (JSPS) fellowship tenable at the National Institute for Materials Science, Tsukuba, Japan (X. S. Fang). The authors thank Drs G. Z. Shen, U. K. Gautam, Y. Uemura, M. Mitome, C. Y. Zhi, C. C. Tang, and Q. Huang for cooperation and kind help.

Notes and references

1 C. N. R. Rao, F. L. Deepak, G. Gundiah and A. Govindaraj, *Prog. Solid State Chem.*, 2003, **31**, 5; E. G. Wang, *J. Mater. Res.*, 2006, **21**, 2767; X. S. Fang and L. D. Zhang, *J. Mater. Sci. Technol.*, 2006, **22**, 1.
2 A. W. Xu, Y. R. Ma and H. Cölfen, *J. Mater. Chem.*, 2007, **17**, 415; L. Li, Y. W. Yang, X. H. Huang, G. H. Li and L. D. Zhang, *J. Phys. Chem. B*, 2005, **109**, 12394; L. Li, Y. W. Yang, G. H. Li and L. D. Zhang, *Small*, 2006, **2**, 548.
3 J. Chen, S. L. Li, Z. L. Tao and F. Gao, *Chem. Commun.*, 2003, 980; X. S. Fang, C. H. Ye, L. D. Zhang, J. X. Zhang, J. W. Zhao and P. Yan, *Small*, 2005, **1**, 422; X. S. Fang and L. D. Zhang, *J. Mater. Sci. Technol.*, 2006, **22**, 721.
4 N. S. Xu and S. E. Huq, *Mater. Sci. Eng., R*, 2005, **48**, 47.
5 S. S. Fan, M. G. Chapline, N. R. Franklin, T. W. Tombler, A. M. Cassell and H. J. Dai, *Science*, 1999, **283**, 512; Z. Xu, X. D. Bai, E. G. Wang and Z. L. Wang, *Appl. Phys. Lett.*, 2005, **87**, 163106; D. Banerjee, S. H. Jo and Z. F. Ren, *Adv. Mater.*, 2004, **16**, 2028.
6 W. I. Milne, K. B. K. Teo, G. A. J. Amaratunga, P. Legagneux, L. Gangloff, J. P. Schnell, V. Semet, V. T. Binh and O. Groening, *J. Mater. Chem.*, 2004, **14**, 933.
7 Q. Wu, Z. Hu, X. Z. Wang, Y. N. Lu, K. F. Huo, S. Z. Deng, N. S. Xu, B. Shen, R. Zhang and Y. Chen, *J. Mater. Chem.*, 2003, **13**, 2024; X. B. Wang, L. Q. Liu, D. B. Zhu, L. Zhang, H. Z. Ma, N. Yao and B. L. Zhang, *J. Phys. Chem. B*, 2002, **106**, 2186; J. Y. Fan, X. L. Wu and P. K. Chu, *Prog. Mater. Sci.*, 2006, **51**, 983.
8 Y. F. Lin, Y. J. Hsu, S. Y. Lu and S. C. Kung, *Chem. Commun.*, 2006, 2391; Y. H. Li, Y. M. Zhao, M. Roe, D. Furniss, Y. Q. Zhu, S. R. P. Silva, J. Q. Wei, D. H. Wu and C. H. P. Poa, *Small*, 2006, **2**, 1026.
9 W. Z. Wang, B. Q. Zeng, J. Yang, B. Poudel, J. Y. Huang, M. J. Naughton and Z. F. Ren, *Adv. Mater.*, 2006, **18**, 3275.
10 D. Moore and Z. L. Wang, *J. Mater. Chem.*, 2006, **16**, 3898.
11 C. Ma, M. Moore, J. Li and Z. L. Wang, *Adv. Mater.*, 2003, **15**, 228; X. S. Fang, C. H. Ye, L. D. Zhang, Y. H. Wang and Y. C. Wu, *Adv. Funct. Mater.*, 2005, **15**, 63.
12 Y. J. Hsu and S. Y. Lu, *Chem. Commun.*, 2004, 2102; J. F. Gong, S. G. Yang, J. H. Duan, R. Zhang and Y. W. Du, *Chem. Commun.*, 2005, 351.
13 S. H. Yu and M. Yoshimura, *Adv. Mater.*, 2002, **14**, 296; D. Moore, Y. Ding and Z. L. Wang, *Angew. Chem., Int. Ed.*, 2006, **45**, 5150.
14 D. F. Moore, Y. Ding and Z. L. Wang, *J. Am. Chem. Soc.*, 2004, **126**, 14372.
15 Y. C. Zhu, Y. Bando, D. F. Xue and D. Golberg, *Adv. Mater.*, 2004, **16**, 831.
16 S. P. Ge, K. L. Jiang, X. X. Lu, Y. F. Chen, R. M. Wang and S. S. Fan, *Adv. Mater.*, 2005, **17**, 56.
17 F. Lu, W. P. Cai, Y. G. Zhang, Y. Li, F. Q. Sun, S. H. Heo and S. O. Cho, *Appl. Phys. Lett.*, 2006, **89**, 231928.
18 A. Wei, X. W. Sun, C. X. Xu, Z. L. Dong, M. B. Yu and W. Huang, *Appl. Phys. Lett.*, 2006, **88**, 213102; X. S. Fang, Y. Bando, C. H. Ye, G. Z. Shen, U. K. Gautam, C. C. Tang and D. Golberg, *Chem. Commun.*, 2007, DOI: 10.1039/b701113j.
19 S. H. Jo, D. Banerjee and Z. F. Ren, *Appl. Phys. Lett.*, 2004, **85**, 1407.
20 X. S. Fang, Y. Bando, G. Z. Shen, C. H. Ye, U. K. Gautam, C. Z. Zhi, P. M. F. J. C. Costa, C. C. Tang and D. Golberg, *Adv. Mater.*, DOI: 10.1002/adma.200700078.
21 K. Kim, S. H. Lee, W. Yi, J. Kim, J. W. Choi, Y. Park and J. I. Jin, *Adv. Mater.*, 2003, **15**, 1618; Y. B. Tang, H. T. Cong, Z. G. Chen and H. M. Cheng, *Appl. Phys. Lett.*, 2005, **86**, 233104.

